AIAA JOURNAL
Vol. 33, No. 6, June 1995

Control of Streamwise Vortices Using Selective Suction

Roy Y. Myose*
Wichita State University, Wichita, Kansas 67260-0044
and
Ron F. Blackwelder†
University of Southern California, Los Angeles, Los Angeles, California 90089-1191

The breakdown of streamwise vortices was controlled using selective suction. A Görtler flowfield was used to produce streamwise vortices emulating turbulent boundary-layer eddies in a steady laminar-like environment. Suction was applied at single locations under the low-speed region between counter-rotating vortex pairs. A suction coefficient two orders of magnitude less than that required for an asymptotic profile was sufficient to significantly delay the breakdown of the vortices. At high-suction rate, however, premature breakdown resulted due to the creation of an additional instability in the spanwise direction. Results suggest that an ideal control method should produce fuller profiles in the normal direction and eliminate the difference between low- and high-speed regions in the spanwise direction.

Nomenclature

A_E	= effective suction area
A_S	= suction area
C_S	= suction coefficient, $Q_S/(A_E U_\infty)$
Q_S	= volumetric flow rate of suction
U_∞	= freestream velocity
V_W	= velocity through wall, Q_S/A_S
x, y, z	= streamwise, normal, and spanwise distance
δ	= boundary-layer thickness

Introduction

SUCTION has been used to manipulate and control boundary layers in many diverse conditions ranging from the delay of transition to the removal of turbulent boundary layers. During the 1960s, test flights of the X-21 aircraft demonstrated the feasibility of maintaining laminar flow over the wing using suction through many small spanwise slots.[1] Recent test flights of a modified F-16XL aircraft using suction through a wing glove to maintain laminar flow suggests a drag reduction on the order of about 8%.

In the past, suction and other control methods have been utilized over entire surfaces without regards to the structure of the boundary layer. That is, the suction has been applied as uniformly as possible over the entire surface. This alters the mean velocity uniformly and gives it a fuller profile. Such profiles (known as the asymptotic suction profile) are more stable and produce a higher critical Reynolds number.[2] Thus, this technique is useful for delaying transition and reducing the overall drag of a body. The fuller profile produces a larger shear stress at the wall which increases the laminar skin friction. However, if the suction can maintain a laminar flow, the skin friction is less than the turbulent case, and the overall drag is reduced. In the turbulent boundary layer, uniform suction and the fuller profile associated with it will always produce a larger shear stress and, hence, increase the drag.

The novel aspect of the present experiment is that the suction (i.e., the control method) is employed selectively. That is, the control is not applied uniformly over the entire flowfield, but, instead, is designed to act selectively on the identifiable eddies (e.g., low-speed streaks). In turbulent bounded shear flows, the growth and breakdown of low-speed streaks are closely associated with the bursting process.[3,4] This method, therefore, requires some advanced knowledge about the eddies themselves (e.g., their location) along with some knowledge of their dynamics. Given such information, the suction can be employed beneficially to interfere with the growth and movement of the eddies and thus interrupt the Reynolds stress production.[5]

Johansen and Smith[6] used small longitudinal cylinders to anchor meandering low-speed streaks to known locations. Roon and Blackwelder[7] used these longitudinal roughness elements combined with suction (selectively) at the wall underneath the same spanwise location as the low-speed streak and found that the number and duration of low-speed streaks decreased. Gad-el-Hak and Blackwelder[8] artificially generated single and periodic hairpin eddies in a laminar boundary layer, and then used a streamwise oriented suction slot to successfully eliminate this hairpin eddy.

In the present experiment, selective suction was employed in an emulated boundary layer to test its effects in a controlled environment. This differs from the turbulent boundary layer used by Roon and Blackwelder[7] (which involves streak identification issues) or the solitary artificially generated structure utilized by Gad-el-Hak and Blackwelder[8] (as opposed to multiple streaks spatially offset in the spanwise direction). The present emulated boundary layer consists of a Görlter instability developing on a concave wall. Swearingen and Blackwelder[4] have shown that the resulting weak streamwise vortices produce elongated low-speed regions analogous to low-speed streaks in turbulent boundary layers. These emulated streaks are steady and, thus, provide a more controlled eddy structure than in the turbulent boundary layer; at the same time, they have normalized scales comparable to the turbulent boundary-layer structure. As the emulated streaks grow downstream, they become unstable and breakdown in a fashion analogous to their counterpart in the turbulent boundary layer. The present experiment also differs from the previous experiments in that suction was applied pointwise through single holes (which would have practical design advantages) rather than a streamwise oriented slot.

Experimental Method

The experiment was conducted in the low-turbulence open return wind tunnel shown schematically in Fig. 1. The test section is 245 cm long in x with a 15 cm in y by 120 cm in z cross section and a 320 cm radius of curvature concave test wall. Detail A of

Received April 6, 1994; presented as Paper 94-2216 at the AIAA 25th Fluid Dynamics Conference, Colorado Springs, CO, June 20–23, 1994; revision received Oct. 19, 1994; accepted for publication Oct. 19, 1994.

*Assistant Professor, Department of Aerospace Engineering. Senior Member AIAA.

†Professor, Department of Aerospace Engineering. Associate Fellow AIAA.

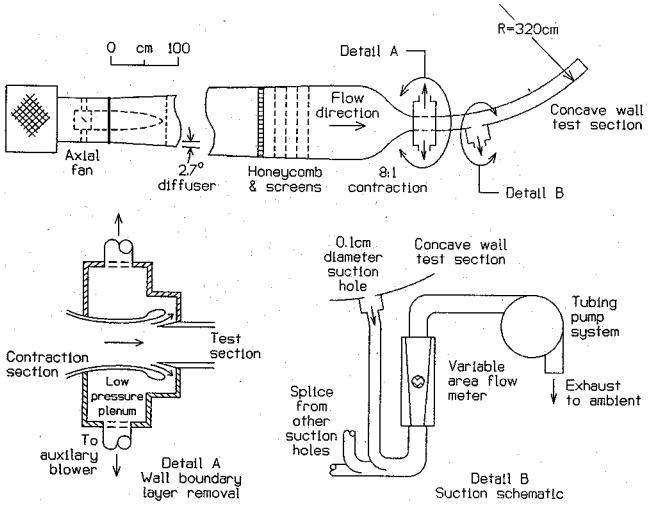

Fig. 1 Experimental setup.

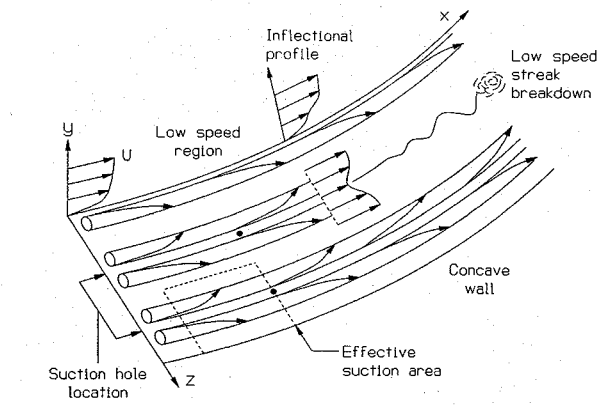

Fig. 2 Experimental situation: uppermost vortex shows inflectional velocity profile, center vortex pair shows inflectional profile in the spanwise direction and development and breakdown of low-speed streak, lowermost vortex pair shows effective suction area. Two of the nine suction holes (depicted by •), each of which is located under the low-speed streak, are shown. Scale in the streamwise x direction is compressed relative to the other directions.

Fig. 1 shows the wall boundary-layer removal device which is used to tangentially remove the tunnel side wall boundary layer. This ensures that the origin of the test section boundary layer begins at the concave wall leading edge. The change in pressure coefficient in the wind tunnel is $\delta(dc_p/dx) \approx -3 \times 10^{-2}$ for $x \geq 70$ cm (i.e., where the measurements were taken). Thus, the pressure gradient is constant and slightly favorably. Additional details of the wind tunnel are given by Swearingen and Blackwelder.[4] A pitot-static tube and pressure transducer system was used to maintain a freestream velocity of $U_\infty = 500$ cm/s $\pm 1\%$ throughout the course of this experiment.

Suction was applied pointwise at $x = 40$ cm through nine individual 0.1-cm-diam holes located at nine different spanwise positions between counter-rotating streamwise vortex pairs (i.e., under the low-speed regions) as depicted in Fig. 2. Air was sucked out of the individual holes via Tygon tubing/Masterflex tubing pump system as shown in detail B of Fig. 1. The suction flow rate was measured by a variable area flow meter. Varying suction rates were applied to explore their effect on the eddy structure. A sheet of smoke was introduced at $x = 22$ cm and $y = 0.14$ cm ($y/\delta_{\text{Blasius}} \approx 0.35$) using the smoke-wire technique.[4] The resulting smoke patterns were then recorded using a charge coupled device (CCD) camera and super-video home system (S-VHS) video system. Streamwise velocity measurements were taken under select conditions by traversing a single sensor hot wire. The standard hot-wire measurement technique[4] was used in this experiment.

The amount of applied suction is defined by the suction coefficient $C_S \equiv V_W/U_\infty$ where V_W is the normal velocity through the wall.[2] In the case of uniform suction, the normal velocity through the wall is then given by $V_W = Q_S/A_S$ where Q_S is the volumetric flow rate of suction and A_S is the applied suction area. Since suction is applied under a very large area in this case, the average velocity through the wall is rather small. In the case of pointwise suction utilized in this experiment, the associated volumetric flow rate is relatively small. However, the velocity through the wall is relatively large due to the fact that suction is applied at a single point through a small hole area. To allow comparison with uniform suction, especially the asymptotic suction profile case, the suction coefficient is defined as $C_S = Q_S/(A_E \cdot U_\infty)$ where A_E is the area over which the suction has an effect. There are two possible schemes for characterizing this effective area. One scheme is to determine the downstream area which the suction affects. This would require determining the downstream location where low-speed streaks break down with and without suction. The region of downstream delay in breakdown would then be used as the effective area. However, it would then be difficult to ascribe a suction coefficient for a case with no delay (i.e., an effective area of zero) as well as cases involving early breakdown. Since the low-speed streak undergoes growth, another scheme for characterizing the effective area is to view the role of suction as reversing (or reducing) the effects of this growth which occurred upstream. This second scheme, as described subsequently, was chosen for the purposes of comparison with the asymptotic suction case.

Although the instability responsible for developing the vortical system in Görtler flow commences close to the leading edge, a small streamwise distance is required before its effect is noticeable. According to Swearingen and Blackwelder,[4] the boundary layer is Blasius-like for at least the first 10 cm. Since the purpose of the suction is to reduce or eliminate the low-speed region that results from the streamwise vortices, the suction holes at $x = 40$ cm try to reverse the effects of the previous 30 cm. Consequently, an effective streamwise suction length of 30 cm was used. Since the average spanwise spacing between low-speed regions is 3.2 cm, the effective suction area A_E is 96 cm^2.

Results and Discussion

Figure 2 depicts the experimental situation. Because of the updraft action between pairs of counter-rotating streamwise vortices removing low-momentum fluid away from the wall, an inflectional velocity profile results in both the normal and spanwise directions. When particulates such as smoke are introduced into this vortical flow system, the smoke coalesces to the low-speed region resulting in a streak-like visual pattern. Downstream, this low-speed streak develops a secondary instability and then breaks down. The suction is applied in this experiment to reduce the instability and delay the breakdown of the low-speed streak. Although many different suction rates were tested, results for three suction coefficients of $C_S = 2.4 \times 10^{-5}$ (optimum), 7.2×10^{-5} (moderate), and 20×10^{-5} (large) are presented in detail. In comparison, the amount of suction (i.e., C_S or Q_S) required for the asymptotic profile[2,7] over a comparable area is more than an order of magnitude larger (see Table 1). It should be noted, however, that this comparison with asymptotic suction should be done with care. In asymptotic suction, the purpose is to maintain laminar flow, and the method used is uniform suction; this is quite different from pointwise suction. As discussed earlier, the velocity through the wall V_w is larger for pointwise suction since the hole diameter (i.e., actual suction area) is small. Although this

Table 1 Suction conditions

Case	$C_S \times 10^{-5}$	Q_S, cm^3/s	V_w/U_∞
Optimum	2.4	1.2[a]	0.29
Moderate	7.2	3.5[a]	0.88
Large	20	9.6[a]	2.44
Asymptotic	300[b]	144[b]	0.003

[a]For an effective suction area of 96 cm^2 which is necessary to affect one typical low-speed streak.
[b]Based on an assumption of comparable effective area.

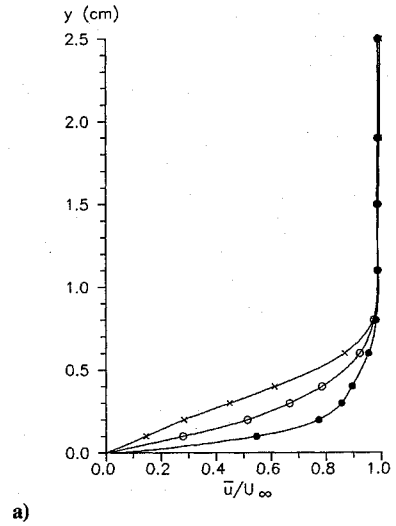

Fig. 3 Time-averaged velocity profile in the normal direction at x = 80 cm for pointwise suction applied at x = 40 cm, z = 8.2 cm; × no suction, ○ $C_S = 7.2 \times 10^{-5}$, ● $C_S = 20 \times 10^{-5}$: a) profile over the low-speed region, z = 8.2 cm and b) profile over the high-speed region, z = 7.0 cm.

suction velocity through the wall may be relatively large locally, the overall suction rates (e.g., Q_S) necessary to affect a given area is much smaller since suction is applied selectively. Measurements were not taken in the immediate vicinity of the suction holes, but farther downstream since the purpose of the present experiment is to determine the effect of selective suction on the breakdown of the low-speed streaks.

Figure 3 shows the velocity profile in the normal direction at spanwise locations over the low- and high-speed regions. The velocity profile for the no suction case in Fig. 3a is inflectional and unstable. When suction is applied, the profile becomes fuller and, therefore, more stable. Although normal profile measurements for optimum suction ($C_S = 2.4 \times 10^{-5}$) were not taken, the missing velocity profile should fall between the no suction and moderate suction cases. Since the suction is applied pointwise in this experiment, the effect of suction is not felt in the high-speed region shown in Fig. 3b, and these profiles remain virtually unchanged.

The smoke wire flow-visualization results, with and without suction, are shown in Fig. 4. Each photograph encompasses a spanwise region including seven low-speed streaks (although the streak at $z = -0.6$ cm is somewhat obscured by the reference centerline). Suction was applied upstream at $x = 40$ cm under these low-speed streaks (and two others outside the photographic field of view). For the no suction case in Fig. 4a, the low-speed streaks develop a sinuous motion instability starting from about $x \approx 115$ cm.

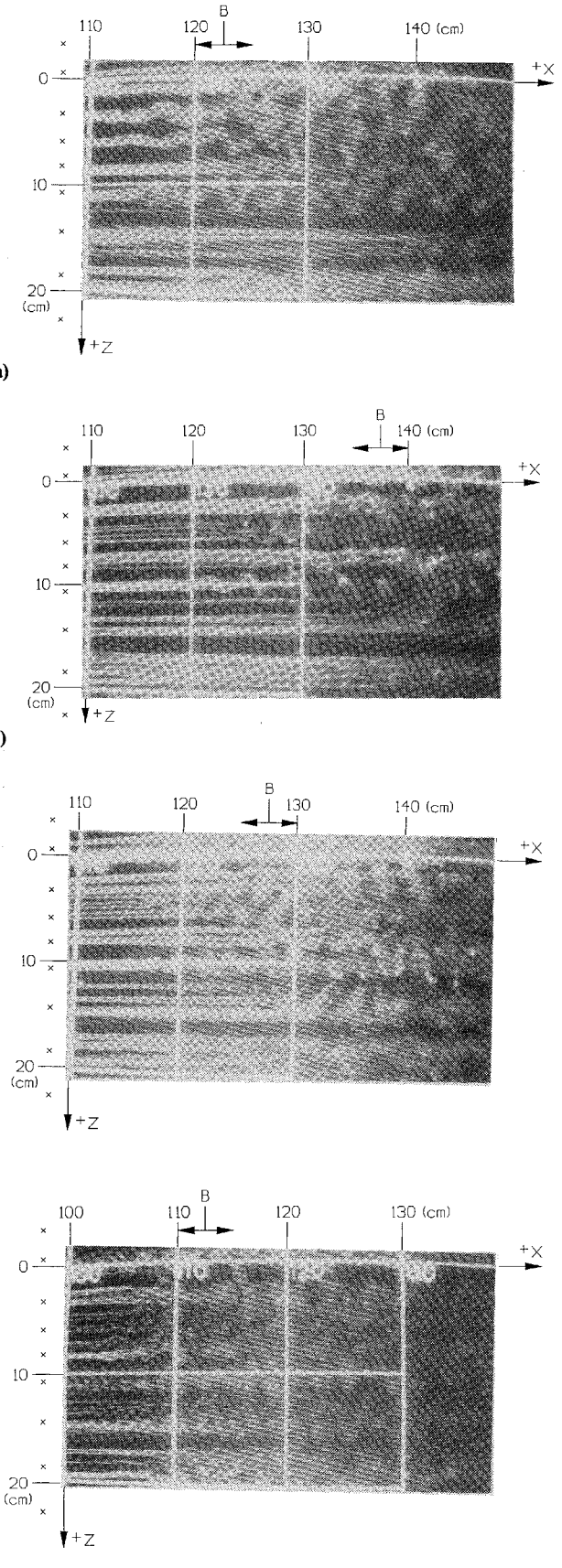

Fig. 4 Smoke wire flow visualization with and without suction, flow direction left to right, horizontal and vertical white reference lines 10 cm apart, suction holes (at z = −3.3, −0.6, 3.3, 5.9, 8.2, 10.7, 14.4, 18.5, and 22.7 cm) indicated by ×. Although hole locations are shown in a), no suction was applied in this case; typical breakdown location for the five upper streaks [i.e., those in the range $-0.6 \leq z$ (cm) ≤ 10.7] is indicated by B: a) no suction case, b) $C_S = 2.4 \times 10^{-5}$, c) $C_S = 7.2 \times 10^{-5}$, and d) $C_S = 20 \times 10^{-5}$.

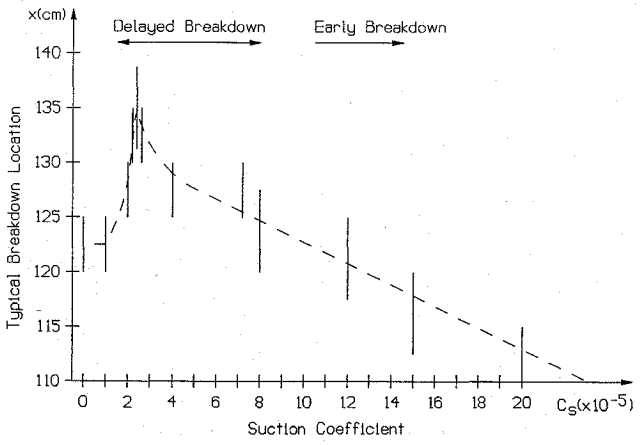

Fig. 5 Typical breakdown location as a function of suction coefficient.

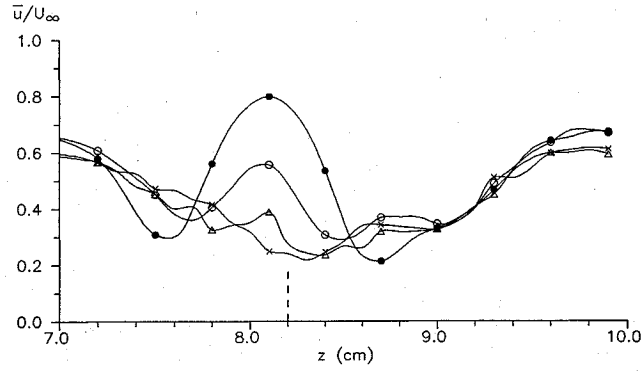

Fig. 6 Time-averaged velocity profile in the spanwise direction at x = 80 cm, y = 0.2 cm, pointwise suction is applied at x = 40 cm, z = 8.2 cm (indicated by the dashed lines); ×, no suction, △ $C_S = 2.4 \times 10^{-5}$, ○ $C_S = 7.2 \times 10^{-5}$, and • $C_S = 20 \times 10^{-5}$.

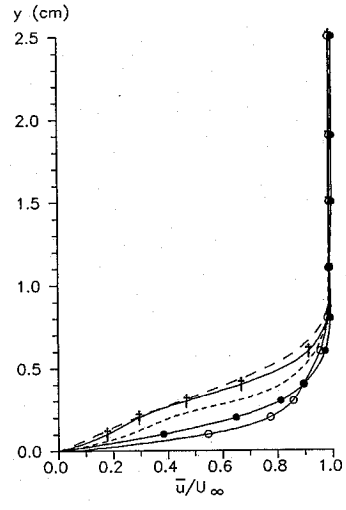

Fig. 7 Time-averaged velocity profile in the normal direction at x = 80 cm. Although not explicity shown, the velocity profile at the high-speed region for the no suction case is quite similar to the velocity profile at z = 7.0 cm for the large suction case (as shown in Fig. 3b): no suction — — low-speed region, z = 8.2 cm and - - - - mid-speed region, z = 7.6 cm; $C_S = 20 \times 10^{-5}$, large suction ○ at z = 8.2 cm, † at z = 7.6 cm, and • at z = 7.0 cm.

This instability leads to the breakdown of the low-speed streaks by $x \approx$ 120–125 cm. For the optimum suction case shown in Fig. 4b, the sinuous motion instability is delayed until $x \approx$ 125–130 cm, and breakdown does not occur until $x \approx$ 135–140 cm. This delaying effect is especially significant in light of the fact that the applied suction rate is extremely small, i.e., about two orders of magnitude smaller than the suction rate required for an asymptotic profile. At a moderate suction rate shown in Fig. 4c, there is a delay of about 5 cm (compared to the no suction case) for the onset of sinuous motion instability and breakdown of the low-speed streak. This is not as significant a delay as the optimum suction case. A closer examination of the flow-visualization results reveal that the smoke in the center of individual low-speed streaks is often nonexistent. The low-speed streaks at $z \approx$ 3 cm and 8 cm in Fig. 4c, for example, have dark smokeless center regions when compared to the same low-speed streaks in Fig. 4a. The smokeless regions may be due to smoke removal by the suction ports. Another possibility is the presence of a local high-speed region since the smoke tends to coalesce in low-speed regions. In Fig. 4d, the photographic field of view shown is 10 cm upstream of the other flow-visualization photographs. It is evident that the high-suction rate has precipitated a premature breakdown of the low-speed streaks. A closer examination of the flow-visualization results for the higher suction rates indicate that the number of low-speed streaks has doubled over the spanwise region where suction was applied as discussed later on.

Figure 5 summarizes the effect of suction rate on the breakdown of the low-speed streaks. These results are based on flow visualizations similar to those shown in Fig. 4. For each suction rate, the range of breakdown locations observed during multiple flow-visualization runs are shown in Fig. 5. A consistent trend in the low-speed streak breakdown location is shown by the figure. The breakdown is delayed farther downstream as the suction rate is increased from zero up through the optimum suction rate of $C_S = 2.4 \times 10^{-5}$. However, as the suction rate is increased beyond optimum, breakdown begins to move upstream. The reason for this early breakdown becomes apparent when the spanwise velocity profile is examined.

The velocity profile in the spanwise direction for the four different cases are shown in Fig. 6. The no suction case indicates that the low-speed streak is centered at about $z \approx$ 8.2 cm. It is evident from the figure that pointwise suction produces a higher speed flow where a low-speed region existed in the no suction case. At moderate suction rate, this higher speed flow at z = 8.2 cm is strong enough to locally impede the coalescence of smoke particulates near the streak center as shown in Fig. 4c. The optimum and moderate suction rate cases produce the higher speed flow in the immediate vicinity of the suction hole without significantly affecting other spanwise regions. At the high-suction rate, the velocity at z = 8.2 cm is higher speed than even the archetypical high-speed regions at z = 7 cm and $z \approx$ 10 cm. Furthermore, the midspan regions of z = 7.6 and 8.7 cm are transformed into low-speed regions with velocities comparable to the no suction case low-speed region. Consequently, for the high-suction rate case, there are twice as many low-speed regions, and the spacing between low-speed streaks (as well as the Görtler vortex wavelength) has thus been halved. Myose and Blackwelder[9] found that a reduction in the Görtler vortex wavelength resulted in early onset of secondary instability and breakdown of the low-speed streaks. Both the wavelength halving and the early breakdown are consistent with the flow-visualization result of Fig. 4d.

A further comparison between the high-suction rate and no suction cases are presented in Fig. 7. High suction transforms the inflectional profile at z = 8.2 cm (long dashed line) into a profile (○) which is fuller than the archetypical high-speed region at z = 7.0 cm (•). In the midspan region (z = 7.6 cm), high suction results in a profile (†) which is more inflectional than the profile in the low-speed region of the no suction case (long dashed line). Swearingen and Blackwelder[4] found that the normal profile became more inflectional in the low-speed region and fuller in the high-speed region as the flow developed downstream and became unstable. This suggests that the flow is highly unstable at high-suction rate. Figure 6 also indicates that spanwise shear ($\partial U/\partial z$) in the profile at high-suction rate is significantly larger than the no suction case. Swearingen and Blackwelder[4] found that inflectional spanwise profiles and large spanwise shear cause flow instability just as inflectional normal profiles do. Therefore, the flow is actually made more unstable when suction is applied at too high a rate. When selective suction is properly applied as in the optimum and moderate suction cases, a fuller, more stable profile is produced in the normal direction

whereas in the spanwise direction the velocity difference between low- and high-speed regions are diminished. In such a case, the onset of sinuous instability and breakdown of the low-speed streak is delayed as illustrated in Fig. 4.

Additional suction methods were attempted to try and obtain further delays in the onset of instability and breakdown. These attempts included the use of larger 0.3-cm-diam holes (at $x = 41$ cm), increasing the number of suction holes from 9 to 27 (0.1 cm diameter at $x = 30$, 40, and 55 cm), and employing a plenum system of 72 holes (0.1 cm diameter at 5-cm intervals between $x = 35$ and 70 cm); however, suction was still applied only under the low-speed streaks. These methods were employed with the idea that suction would be applied more gently and over a longer downstream distance. None of these methods resulted in further delays of breakdown onset. Since the low-speed streak is located directly above the suction port (see Fig. 2), the effect of suction will be felt more strongly in the normal direction than in the spanwise direction. To reduce the spanwise velocity difference between the high- and low-speed regions and, hence, reduce the spanwise inflectional profile, additional suction ports would need to be employed with a spanwise displacement. This application of selective suction would alleviate the additional spanwise inflection points introduced by the strong suction (see Fig. 6) and possibly delay the breakdown farther downstream. An alternative approach would be to apply suction in the low-speed region and injection in the high-speed region as suggested by Gad-el-Hak and Blackwelder.[8] Neither of these methods was attempted during the course of this experiment.

Conclusions

Selective suction has a significant effect upon the low-speed regions and their breakdown according to the present experiment. Results indicate that suction should be applied in such a manner that a more stable fuller profile is promoted in the normal direction without generating an additional instability in the spanwise direction. Consequently, an ideal control method should produce a fuller profile in the normal direction and eliminate the difference between low- and high-speed regions in the spanwise direction. At optimum suction rates, selective suction successfully delayed the breakdown of the low-speed region, and by analogy should reduce the production of turbulent energy in a turbulent boundary layer. The main conclusion from this study is that the suction rate necessary for delay of breakdown was significantly reduced (by about two orders of magnitude) by selective application of suction at judiciously chosen spanwise locations.

Acknowledgments

This work was sponsored by the Office of Naval Research under Contract N00014-92-J1062 monitored by L. P. Purtell. This support is gratefully acknowledged. The authors acknowledge the assistance of Depei Liu for the pressure gradient information of the Görtler wind tunnel.

References

[1]Whites, R. C., Suddereth, R. W., and Wheldon, W. G., "Laminar Flow Control on the X-21," *Astronautics and Aeronautics*, Vol. 4, July 1966, pp. 38–43.

[2]Schlichting, H., *Boundary-Layer Theory*, 7th ed., McGraw–Hill, New York, 1979, pp. 383–388, 506–510.

[3]Robinson, S. K., "Coherent Motions in the Turbulent Boundary Layer," *Annual Review of Fluid Mechanics*, Vol. 23, 1991, pp. 601–639.

[4]Swearingen, J. D., and Blackwelder, R. F., "The Growth and Breakdown of Streamwise Vortices in the Presence of a Wall," *Journal of Fluid Mechanics*, Vol. 182, Sept. 1987, pp. 255–290.

[5]Blackwelder, R. F., "Some Ideas on the Control of Near-Wall Eddies," AIAA Paper 89-1009, March 1989.

[6]Johansen, J. B., and Smith, C. R., "Effects of Cylindrical Surface Modifications on Turbulent Boundary Layers," *AIAA Journal*, Vol. 24, No. 7, 1986, pp. 1081–1087.

[7]Roon, J. B., and Blackwelder, R. F., "The Effects of Longitudinal Roughness Elements and Local Suction upon the Turbulent Boundary Layer," *Structure of Turbulence and Drag Reduction*, edited by A. Gyr, Springer–Verlag, Zurich, 1990.

[8]Gad-el-Hak, M., and Blackwelder, R. F., "Selective Suction for Controlling Bursting Events in a Boundary Layer," *AIAA Journal*, Vol. 27, No. 3, 1989, pp. 308–314.

[9]Myose, R. Y., and Blackwelder, R. F., "Controlling the Spacing of Streamwise Vortices on Concave Walls," *AIAA Journal*, Vol. 29, No. 11, 1991, pp. 1901–1905.